ACS OMEGA

Open Access

http://pubs.acs.org/journal/acsodf

Article

Integrated Pharmaco-Bioinformatics Approaches and Experimental Verification To Explore the Effect of Britanin on Nonalcoholic Fatty Liver Disease

Chengyun Dou, Hongbo Zhu, Xia Xie, Cuiqin Huang, and Chuangjie Cao*

Cite This: *ACS Omega* 2024, 9, 8274−8286

Read Online

ACCESS | Metrics & More | Article Recommendations

ABSTRACT: Nonalcoholic fatty liver disease (NAFLD) is a prevalent global liver disorder, posing substantial health risks. Britanin, a bioactive sesquiterpene lactone extracted from Inula japonica, has demonstrated antidiabetic, hypolipidemic, and hepatoprotective attributes. Nonetheless, the precise impact of Britanin on NAFLD and the intricate biological mechanisms underpinning this interaction remain unexplored. We integrated computer-aided methods to unearth shared biological targets and signaling pathways associated with both Britanin and NAFLD. A network was constructed by compiling putative targets associated with Britanin and NAFLD, followed by a stringent screening of key targets and mechanisms through protein−protein interaction analysis along with GO and KEGG pathway enrichment analyses. Molecular docking was integrated as an evaluation tool, culminating in the identification of HO-1 as the pivotal therapeutic target, showcasing a satisfactory binding affinity. The primary mechanism was ascribed to biological processes and pathways linked to oxidative stress, as evidenced by the outcomes of enrichment analyses. Of these, the AMPK/SREBP1c pathway assumed centrality in this mechanism. Furthermore, in vivo experiments substantiated that Britanin effectively curtailed NAFLD development by ameliorating liver injury, modulating hyperlipidemia and hepatic lipid accumulation, and alleviating oxidative stress and apoptosis. In summary, this study demonstrates the potential of Britanin as a promising therapeutic drug against NAFLD.

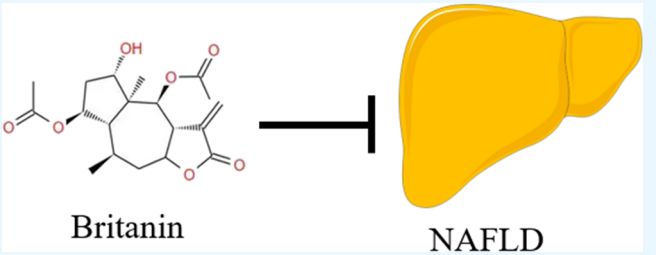

INTRODUCTION

Nonalcoholic fatty liver disease (NAFLD) is a prevalent liver disease worldwide, affecting approximately 25% of the population.[1,2] Initially regarded as a benign condition primarily associated with obesity, recent research has revealed the intricate nature of NAFLD. Numerous studies have demonstrated an elevated risk of mortality associated with NAFLD.[3,4] Furthermore, even the presence of simple steatosis can ultimately lead to increased all-cause mortality due to the progressive nature of the disease over long-term follow-up periods.[5,6] NAFLD encompasses a spectrum of clinical manifestations, ranging from simple steatosis (referred to as fatty liver) to hepatic fibrosis and nonalcoholic steatohepatitis.[7,8] These conditions are associated with an increased risk of liver-related complications including hepatocellular carcinoma, liver failure, and cirrhosis. Additionally, NAFLD is closely linked to significant extra-hepatic manifestations, such as diabetes, dyslipidemia, and cardiovascular disease, further exacerbating its disease burden.[9−14] Consequently, it is imperative to recognize that the effective treatment of this disease would yield substantial benefits for healthcare.

Recently, growing interest in Oriental medicine has prompted a surge in research on natural compounds that exhibit potential for treating inflammatory diseases. Inula japonica Thunb, a frequently utilized medicinal plant in traditional Chinese medicine, has gained recognition for its ability to regulate spleen, liver, lung, and stomach function, as well as its potential in preventing abortion.[15,16] Britanin (Bri) is a bioactive sesquiterpene lactone mainly found in plants like *Inula britannica*, *Inula japonica*, and *Inula linearifolia* Turcz., and it belongs to the category of pharmacologically active phytochemicals.[17,18] *Inula britannica* extract has shown antioxidant and hepatoprotective properties in vitro.[19] Moreover, Wu et al. reported that Britanin functions as a protective phytochemical against ischemic brain injury in a rat model of middle cerebral artery occlusion-reperfusion (MCAO/R).[20] Kim et al. demonstrated that Britanin mitigates airway inflammation induced by ovalbumin in a murine model of asthma.[21] In addition, contemporary pharmacological investigations have revealed its

Received: November 10, 2023
Revised: January 16, 2024
Accepted: January 23, 2024
Published: February 9, 2024

multifaceted effects, encompassing antidiabetic, hypolipidemic, and hepatoprotective activities. In detail, Britanin exhibited antiadipogenic properties by reducing intracellular lipid accumulation and modulating the expression of markers associated with lipogenesis and adipogenesis.[22] Britanin, when administered orally, notably decreased blood lipid and glucose levels in diabetic mice, suggesting the antidiabetic and hypolipidemic effects of Britanin.[23] Nevertheless, the potential of Britanin in alleviating NAFLD has yet to be elucidated. Hence, the objective of this study is to investigate the potential protective effect of Britanin against NAFLD and elucidate the underlying mechanism using a combination of pharmacobioinformatics approaches and experimental verification.

MATERIALS AND METHODS

Screening and Identification of Britanin Targets. The potential targets of Britanin were obtained using SymMap, TCMID, and TCMSP databases. The PubChem database (https://pubchem.ncbi.nlm.nih.gov/) was utilized to acquire single large flowers, inula Britanin 2d structure. The SwissTargetPrediction database (http://www.swisstargetprediction.ch/) was further used to predict the potential targets of Britanin. In the SwissTargetPrediction tool, it is hypothesized that the top 15% of results carry a 75% likelihood of representing the compound's target. Consequently, the initial 15 results from SwissTargetPrediction were chosen. The *Z*-score for network proximity was derived from the mean and standard deviation of random distances. Comparing results from the PharmMapper database, the *Z*-score exhibits a superior confidence interval and statistical significance compared to the 'Fit score', aligning with it. Results with *Z*-score > 0 was considered significant, while a negative *Z*-score indicated insignificance. Additionally, a higher *Z*-score correlates with a more favorable combination of compound molecules and protein targets. Within TargetNet, outcomes with a probability (Prob) ≥ 0.9 (http://targetnet.scbdd.com) were deemed reliable targets for active ingredients. Hence, to enhance result confidence, Prob ≥ 0.9 and *Z*-score > 0 were chosen as effective criteria in this study.

Acquisition of Disease Targets. In gene expression omnibus (GEO) databases (https://www.ncbi.nlm.nih.gov/geo/), the transcriptome chip data related to "nonalcoholic fatty liver disease" was downloaded, and the screening criteria were as follows: The key word is "nonalcoholic fatty liver disease" and "human beings". Then, the bioconductor R package in R software was used to rectify the background, normalize, and calculate the expression value of the chip data. The differentially expressed mRNAs between the two groups were calculated using the limma package. The *P* value < 0.05 and (|log2 FC| ≥ 0.58) variation range ≥ 1.50 were set as the criteria for screening differential genes in which log2FC ≥ 0.58 represented upregulated mRNA expression, and log2FC ≤ −0.58 represented downregulated mRNA expression. Subsequently, differentially expressed genes (DEGs) related to NAFLD were obtained. The DEGs obtained from screening were used to generate a heatmap and perform clustering analysis using the heatmap package. The *P*-values in the differentially processed data were transformed to −log10 scale, and based on the log2FC values, the −log10 (*P*-value) was grouped into upregulated DEGs, downregulated DEGs, and DEGs with no statistical significance. The processed data was then imported into R to create a volcano plot. Additionally, by searching the "nonalcoholic fatty liver disease" in the Genecards (https://www.genecards.org/) database, disease targets related to NAFLD were obtained. The acquired targets were merged and deduplicated and then matched with validated human target gene names using the Uniprot database.

Gene Set Enrichment Analysis. Using the clusterprofiler R package, gene set enrichment analysis (GSEA) was performed on the gene sets from the aforementioned NAFLD data set. The "hallmark gene sets" were selected for comparison, aiming to explore the biological functions played by the gene sets between NAFLD and normal tissues.

Identification of Common Targets between Britanin and NAFLD and Construction of a PPI Network. To elucidate the interactions between NAFLD-related targets and the potential targets of Britanin, the R language (https://www.r-project.org/) software and the Perl programming language were utilized. The disease targets and Britanin targets were intersected using Venny 2.1 software (http://bioinfogp.cnb.csic.es/tools/venny/index.html) to generate a Venn diagram. The STRING database (https://string-db.org/) was used to construct separate protein−protein interaction (PPI) networks for the shared targets. To ensure data reliability, we specifically chose PPI data related to "*Homo sapiens*" with a confidence score equal to or greater than 0.7 (classified as highest confidence: ≥ 0.9, high: ≥ 0.7, medium: 0.4−0.7, low: < 0.4). These data were utilized for constructing the PPI network, and subsequently, we extracted the largest connected component. Finally, the acquired data set was imported into the Cytoscape software for the purpose of visualizing and analyzing key targets.

GO Biological Function and KEGG Pathway Enrichment Analysis. The shared targets between Britanin and NAFLD were subjected to gene ontology (GO) analysis using the clusterProfilerGO.R package in R language (https://www.r-project.org/) and Perl programming language. We established a threshold of an adjusted *P*-value < 0.05, and the ggplot2 package was employed to visualize the outcomes of significant enrichment. GO analysis serves as the primary method for characterizing the functions of gene products, encompassing biological process (BP), molecular function (MF), and cellular component (CC). Additionally, the clusterProfilerKEGG.R package was employed for KEGG pathway enrichment analysis. Furthermore, the pathview package was utilized to visualize the corresponding signaling pathways. By analyzing the enrichment factor values, the extent of enrichment in key pathways was determined, aiming to explore the potential biological functions and signaling pathway mechanisms of Britanin in treating NAFLD.

Core Target Relative Expression and ROC Evaluation. The expression matrix data related to NAFLD was retrieved and downloaded from the GEO database. This data set encompasses the transcriptome expression matrix file specifically for NAFLD. Subsequently, utilizing the ggpubr package, perform an analysis of the relative expression levels of the core target genes within the NAFLD expression data, previously selected during the preliminary screening. Additionally, a boxplot represents the relative expression levels of these core target genes. Next, the standardized NAFLD-core target gene expression data are merged with the clinical data of NAFLD. Finally, R language packages such as survival, caret, glmnet, survminer, and survival receiver operating characteristic (ROC) are utilized to construct ROC curves for the core genes associated with NAFLD.

Molecular Docking Verification. To validate the interaction between Britanin and the core proteins, we performed molecular docking was performed. The chemical structures of

https://doi.org/10.1021/acsomega.3c08968
ACS Omega 2024, 9, 8274−8286

active compounds were downloaded from the PubChem database (https://pubchem.ncbi.nlm.nih.gov/). Using Chem3D software, corresponding 3D structures were created and exported in the mol2 format. The protein structures of the core proteins were obtained from the PDB database (http://www.rcsb.org/). The protein was processed by using PyMOL software by removing water molecules and phosphate groups. AutoDockTools 1.5.6 software was used to convert the drug's active compounds and the protein gene files from the pdb format to pdbqt format and identify the active binding site. Finally, the Vina script was executed to calculate the molecular binding energy and display the results of molecular docking. Discovery Studio 2019 was also used to identify the docking sites and calculate the flexible binding LibDockScore. The output of the molecular docking results was imported into PyMOL software for visualization of the molecular docking conformations. A binding energy less than 0 indicates spontaneous binding between the ligand and receptor. When Vina binding energy is ≤ -5.0 kcal mol^{-1} and LibDockScore >100, it suggests a stable docking interaction. The 3D and 2D representation of the ligand−receptor complex was displayed to assess the reliability of the bioinformatics analysis prediction.

Animal Experiments. A total of 32 six-week-old C57BL/6J mice were used as animal models, purchased from Changzhou Cavens Experimental Animals Co., Ltd. They were housed in the SPF-grade barrier system at the Animal Facility of the University of south China. After 1 week of acclimatization, the mice were randomly divided into four groups, with eight mice per group, as follows: (1) control group: fed with regular diet; (2) model group: fed with a high-fat diet; (3) low-dose drug group: fed with a high-fat diet + Bri (10 mg/kg); (4) high-dose drug group: fed with a high-fat diet + Bri (20 mg/kg). After 8 weeks of high-fat diet feeding, the mice in the drug groups were subjected to gavage administration of Bri for 6 weeks. After completion of drug administration, the mice were euthanized for sample collection. First, the animals were monitored daily, and when they reached specific humane end points, they were euthanized using pentobarbital sodium. These humane end points included signs such as nose bleeding, skin lesions, breathing difficulties, prostration, considerable loss in body weight, rotational movement, and a decrease in body temperature. Then, blood samples were obtained, and the abdominal cavity was opened to collect liver samples from the mice. All procedures were carried out in conformity with the Animal Care Guidelines of the University of South China and the Institutional Animal Ethics Committee for the use of experimental animals.

Biochemical Analysis. Blood samples were collected from the mice and centrifuged at 3000*g* for 15 min to obtain serum for analysis of four lipid parameters (total cholesterol, triglycerides, HDL cholesterol, and LDL cholesterol) and two liver function markers (ALT and AST) levels. The lipid and liver function assay kits were purchased from Solaibao Biotechnology Co., Ltd., and the measurements were conducted following the instructions provided in the kit manuals.

Determination of Body Weight, Food Intake, and Liver Fat Weight in Mice. After the intervention with Britanin, the body weight and food intake of the mice were measured and recorded every 2 days. After the mice were euthanized, the livers were extracted, photographed, and weighed using an analytical balance.

Histopathological Examination. To observe pathological changes in the liver tissue of mice, we performed histological staining. The liver tissues were fixed and embedded in the OCT compound for frozen sectioning using a cryostat. Oil Red O staining was performed to assess lipid accumulation in the liver. Additionally, the liver tissues were fixed in paraformaldehyde, embedded in paraffin, and sectioned. Hematoxylin and eosin (HE) staining and Masson's trichrome staining were conducted to evaluate general tissue morphology and fibrosis, respectively.

Detection of Oxidative Stress-Related Indexes. Mouse serum was collected, and the levels of malondialdehyde (MDA), superoxide dismutase (SOD), and glutathione peroxidase (GSH-Px) in the serum were measured following the instructions provided in the assay kit.

Immunohistochemistry. After fixation of the liver tissue with paraformaldehyde, paraffin sections were prepared. Immunohistochemical staining was performed using the corresponding primary antibodies, followed by incubation with horseradish peroxidase (HRP)-conjugated secondary antibodies. 3, 3′-diaminobenzidine (DAB) staining was conducted using a DAB kit, followed by counterstaining with hematoxylin. The stained sections were observed under a microscope.

Western Blot Assay. 100 mg portion of liver tissue was homogenized in a lysis buffer to obtain a protein extraction. The total protein extract was obtained after centrifugation. The protein concentration was measured by using a BCA assay kit. SDS-PAGE was employed for protein electrophoresis. Subsequently, the proteins were transferred to a PVDF membrane by using the wet transfer method. The membrane was then blocked and incubated with the primary antibody overnight on a shaker at 4 °C. After the membrane was washed, it was incubated with the secondary antibody and finally visualized. Primary antibodies include AMPK (dilution ratio 1:1000, ab3759, Abcam), pAMPK (dilution ratio 1:1000, ab92701, Abcam), SREBP-1c (dilution ratio 1:1000, ab28481, Abcam), HO-1 (dilution ratio 1:1000, ab13243, Abcam), Caspase3 (dilution ratio 1:1000, ab32351, Abcam), Bcl-2 (dilution ratio 1:1000, ab32124, Abcam), Bax (dilution ratio 1:1000, ab32503, Abcam), and β-actin (dilution ratio 1:2000, ab8227, Abcam). Secondary antibodies were HRP-labeled Goat Anti-Mouse IgG (H + L) (dilution ratio of 1:1000, ab150116, Abcam) and HRP-labeled Goat Anti-Rabbit IgG (H + L) (dilution ratio of 1:1000, ab6721, Abcam). The protein bands were visualized by a Tanon 5500 Imaging System (Tanon Technology Co. Ltd., Shanghai, China).

Statistical Analysis. All experimental data are presented as mean ± standard deviation (mean ± SD). Student's *t* test was used for data comparison between two groups, and $P < 0.05$ was considered statistically significant. In the realm of network pharmacology and bioinformatics analysis, R software was utilized to handle extensive data sets. GraphPad Prism 8.01 and SPSS 24.0 software were used for data visualization and statistical analysis.

RESULTS

Identification of Potential Targets for Britanin. By searching the SymMap, TCMID, and TCMSP databases, a total of seven target proteins corresponding to the drug were identified. In addition, SwissTargetPrediction predicted 108 potential target proteins for Britanin. Combining these results were combined, a total of 112 potential target proteins for Britanin were identified.

Target Screening for NAFLD. The filtering criteria were set as follows: (1) NAFLD and (2) human. Our study originated from the GSE63067 chip data set, which included 99 patients

https://doi.org/10.1021/acsomega.3c08968
ACS Omega 2024, 9, 8274−8286

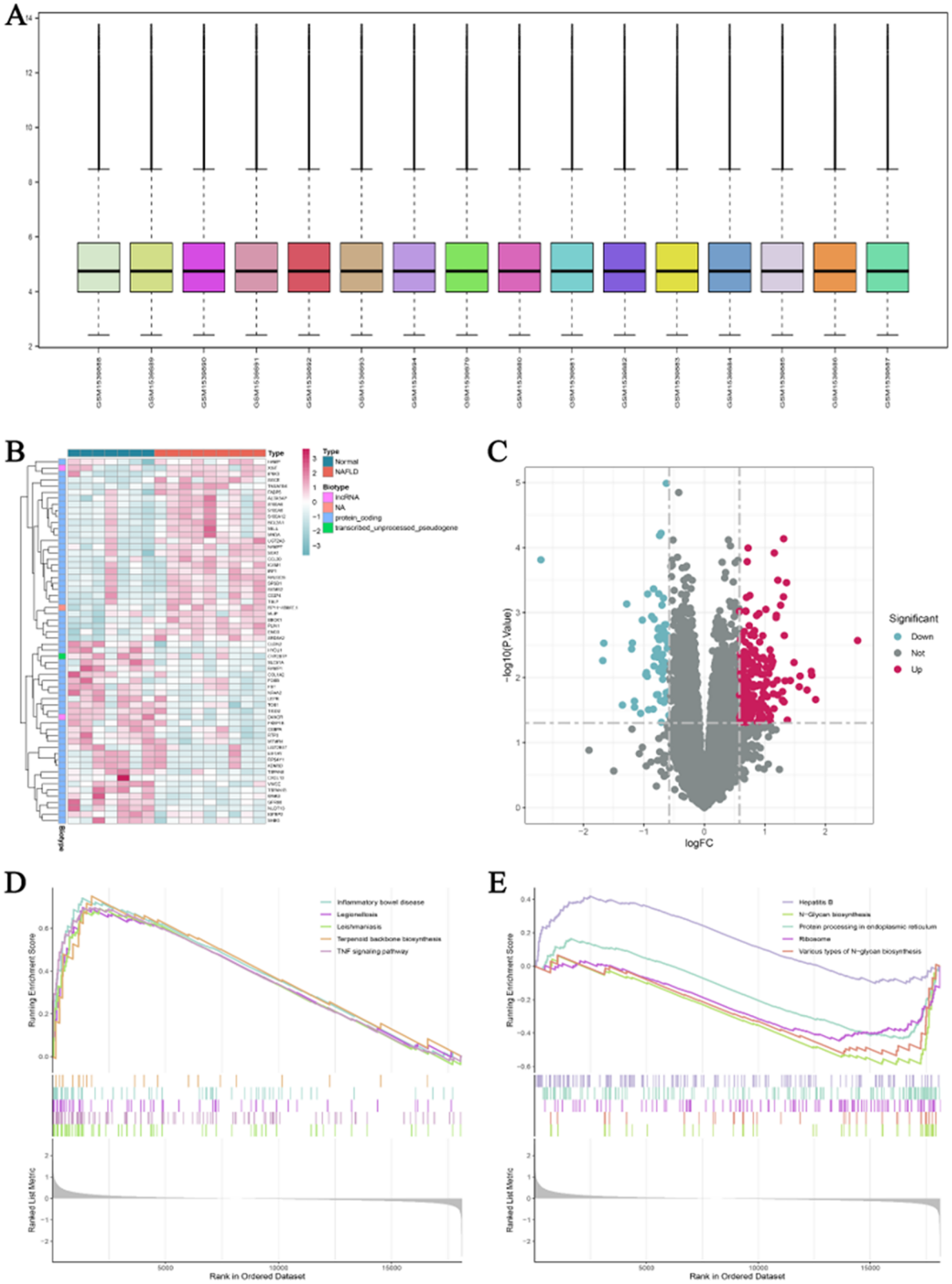

Figure 1. Target selection for NAFLD. (A) Distribution of standardized samples from the GSE63067 data set. (B) Heatmap of DEGs in GSE63067. (C) Volcano plot illustrating DEGs in GSE63067. (D) Gene set enrichment analysis (GSEA) of the upregulated gene set in GSE63067. (E) Gene set enrichment analysis (GSEA) of the downregulated gene set in GSE63067.

with NAFLD and 7 healthy adults. After data background correction and normalization, the sample distribution is shown in Figure 1A. Based on the criteria of *P*-value (<0.05) and expression fold change (≥1.50 or |log2FC| ≥ 0.58), a total of 270 differentially expressed mRNAs were identified in the GSE63067 data set, including 202 upregulated mRNAs and 68 downregulated mRNAs. As shown in Figure 1B, heatmaps of the differentially expressed coding RNAs were generated, with red

https://doi.org/10.1021/acsomega.3c08968
ACS Omega 2024, 9, 8274−8286

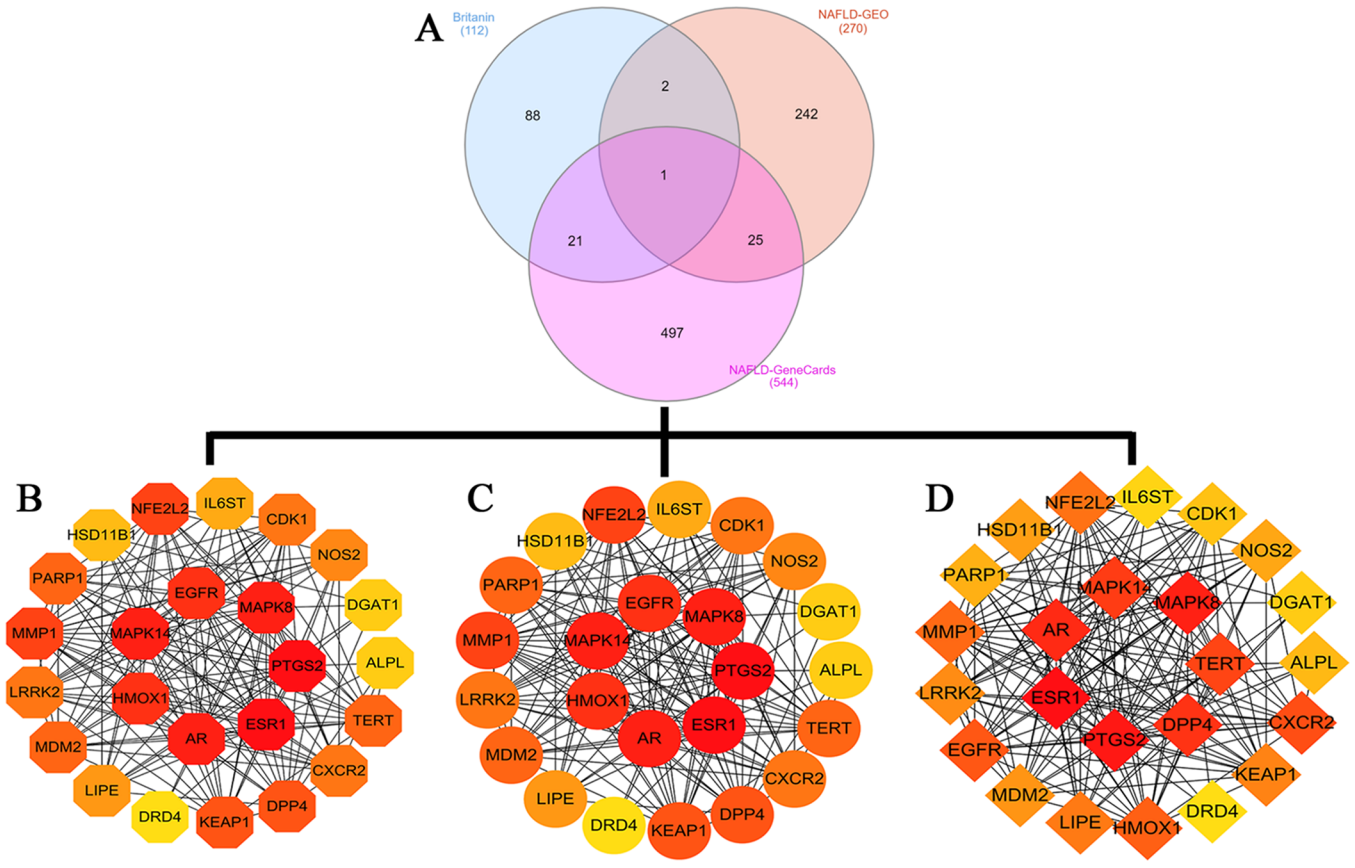

Figure 2. Core gene network. (A) Venn diagram depicting potential core targets of Britanin in NAFLD treatment. (B) Distribution of core targets based on degree centrality. (C) Distribution of core targets based on closeness centrality. (D) Distribution of core targets based on betweenness centrality.

indicating upregulated gene expression and blue indicating downregulated gene expression. The *P*-values from the differential analysis of the chip data were transformed into −log10 scale, and based on log2FC, the −log10 (*P*-value) was grouped into upregulated DEGs, downregulated DEGs, and non-significant DEGs. The processed data was imported into R to generate a volcano plot, as shown in Figure 1C. By sorting the DEGs in NAFLD according to log2FC, GSEA analysis revealed significant enrichments. As shown in Figure 1D, the upregulated gene set in NAFLD, compared to healthy adults, showed significant enrichment in pathways such as inflammatory bowel disease, legionellosis, leishmaniasis, terpenoid backbone biosynthesis, and the TNF signaling pathway. The downregulated gene set exhibited significant enrichment in pathways including hepatitis B, N-glycan biosynthesis, protein processing in the endoplasmic reticulum, ribosome, and various types of N-glycan biosynthesis (Figure 1E).

Screening of Common Targets. By searching the Genecards database with a relevance score threshold of ≥10 for "nonalcoholic fatty liver disease", a total of 544 proteins associated with NAFLD-related diseases were obtained. The 112 potential target proteins of the active compounds were separately compared with 270 NAFLD-related targets and 544 proteins associated with NAFLD-related diseases. Using the online Venn diagram tool InteractiVenn, the matched mappings identified 24 potential targets for the treatment of NAFLD by Britanin. These include LRRK2, CXCR2, DPP4, HO-1, MAPK8, and MAPK14. As shown in Figure 2A, the Venn diagram illustrates the intersection of the active compound and disease targets. Furthermore, the Cytoscape 3.7.2 software results showed a common target network for Britanin and NAFLD. The top 10 core targets were selected based on Degree, Closeness, and Betweenness values (Figure 2B–D). These core targets included LRRK2, ESR1, AR, MAPK8, MAPK14, HO-1, EGFR, MMP1, NFE2L2, and DPP4.

Results of GO and KEGG Enrichment Analysis. The bioconductor and clusterProfiler packages in R were used to perform GO and KEGG enrichment analysis on the 24 potential targets of Britanin for the treatment of NAFLD. The results of the GO analysis revealed that the potential target genes were primarily enriched in BPs, such as cellular response to chemical stress, response to metal ion, and cellular response to oxidative stress. In terms of CCs, the enrichment was observed in the membrane raft, membrane microdomain, and caveola, among others. The MFs were predominantly associated with transcription cofactor binding, transcription coactivator binding, and virus receptor activity (Figure 3A,B). Furthermore, the KEGG analysis identified significant enrichment in pathways such as endocrine resistance, the relaxin signaling pathway, fluid shear stress and atherosclerosis, and the IL-17 signaling pathway (Figure 3C,D).

ROC Curve Construction. To further elucidate the expression changes of the 24 intersecting genes in NAFLD, we downloaded relevant gene expression data for NAFLD from GEO. Using the ggpubr package, we analyzed the relative expression levels of the 24 DEGs and generated a boxplot (Figure 4A). The results showed that LRRK2, CXCR2, DPP4, HO-1, MAPK8, and MAPK14 exhibited significantly higher

https://doi.org/10.1021/acsomega.3c08968
ACS Omega 2024, 9, 8274−8286

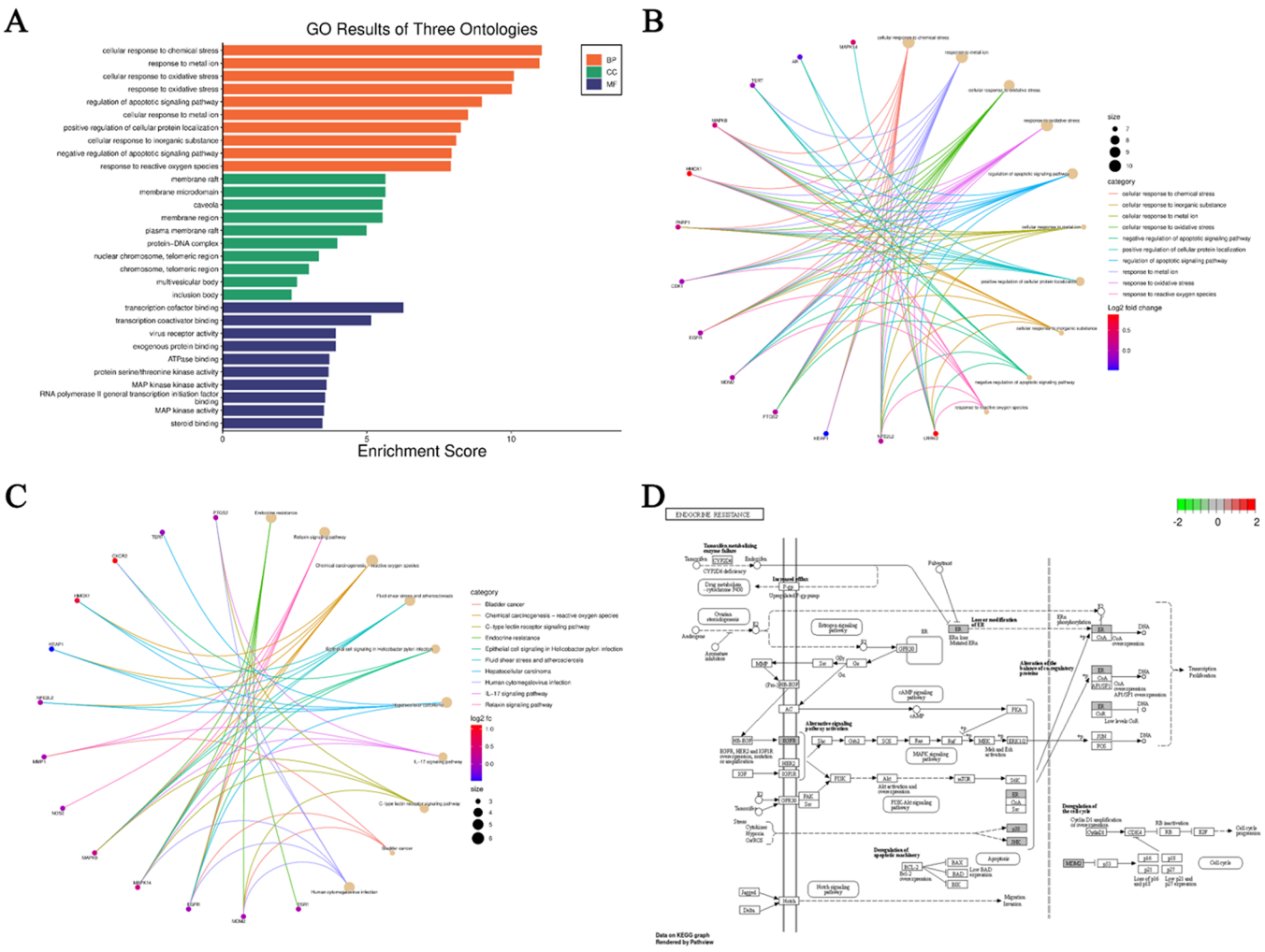

Figure 3. Enrichment analysis. (A) Bar chart depicting GO functional analysis results. (B) Chord diagram illustrating enriched GO terms. (C) Chord diagram illustrating enriched KEGG pathways. (D) Schematic representation of the endocrine resistance signaling pathway.

expression in NAFLD tissues from the GSE63067 data set ($P < 0.05$). Therefore, we performed ROC curve analysis for these six target genes to evaluate their sensitivity and specificity in diagnosing NAFLD. As shown in Figure 4B, the area under the curve values for LRRK2, CXCR2, DPP4, HO-1, MAPK8, and MAPK14 in the GSE63067 data set were all greater than 0.80, suggesting good diagnostic significance.

Results of Molecular Docking. Based on the network pharmacology and bioinformatics analysis, the interaction between Britanin and the core targets of NAFLD, including LRRK2, CXCR2, DPP4, HO-1, MAPK8, and MAPK14, was validated through molecular docking. The 3D structure of Britanin was generated using Chem3D software and saved in mol*2 format. The 3D structures of the core proteins, LRRK2, CXCR2, DPP4, HO-1, MAPK8, and MAPK14, were downloaded from the PDB database and saved in a pdb format. The AutoDockTools 1.5.6 software was used to convert the ligand and target proteins into pdbqt format, and active pockets (binding sites formed by hydrogen bonds, H−π bonds, or π−π bonds with one or more amino acid residues) were identified. The Vina script was executed to calculate the binding energies of the ligand−receptor complexes. The results, presented in Table 1, demonstrated that the binding energies between Britanin and the core proteins LRRK2, HO-1, and MAPK8 were all below −5.0 kcal·mol^{-1}, with RMSD values less than 2.00, indicating stable binding. Additionally, using Discovery Studio 2019 software, molecular docking was performed between the active compound and its corresponding target proteins, and LibDockScores were calculated (Table 1). Based on Table 1, Britanin formed semiflexible docking with the respective core proteins LRRK2, CXCR2, DPP4, HO-1, MAPK8, and MAPK14, and docking sites were successfully identified. Among them, the docking model between the active compound and the core protein HO-1 had a LibDockScore greater than 100. Considering the RMSD, chemical energy, and docking scores, the docking complex formed between Britanin and the core protein HO-1 was the most stable, followed by the complex with the core protein MAPK8. Different core proteins and different active molecules form distinct docking complexes due to the formation of different hydrogen bonds and hydrophobic interactions at specific amino acid residues. Finally, the compound results obtained from Vina were imported into PyMOL and Discovery Studio 2019 software for 3D and 2D molecular docking visualizations, as shown in Figure 5.

Britanin Protects against NAFLD in High-Fat Diet-Fed Mice by Attenuating Liver Injury. Next, we explored the in vivo effects of Britanin on NAFLD. Compared to the normal control group, mice in the high-fat group showed significant increases in body weight, liver weight, and liver index, indicating successful modeling of NAFLD. Importantly, compared to the

https://doi.org/10.1021/acsomega.3c08968
ACS Omega 2024, 9, 8274−8286

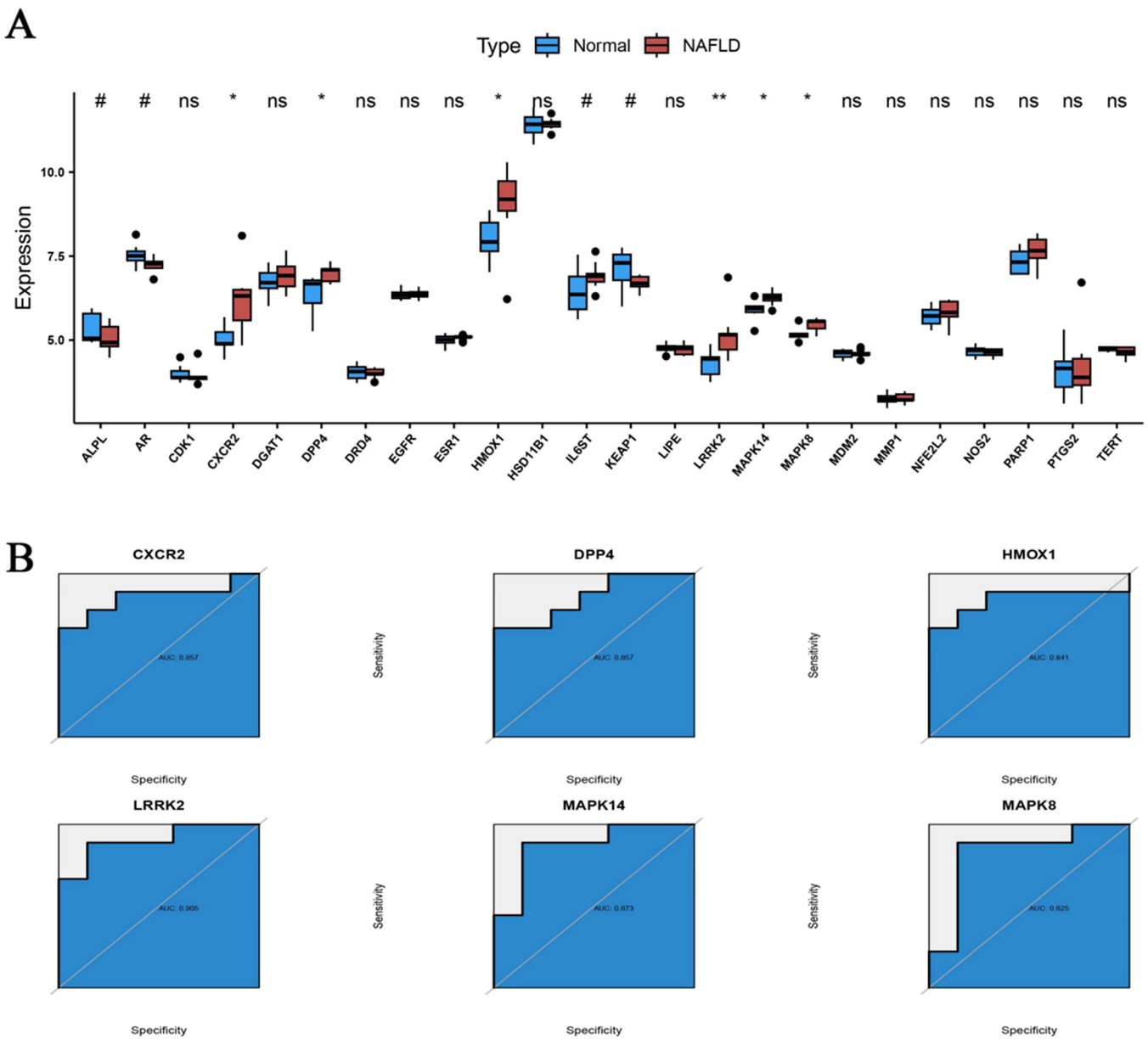

Figure 4. Relative gene expression and ROC model construction. (A) Relative expression levels of core genes in GSE63067 data set. (B) ROC model for core DEGs in GSE63067 samples.

Table 1. Results of Molecular Docking Using Autodock-Vina and Discovery Studio 2019

structural domain	compound	Vina (kcal mol^{-1})	RMSD	DS (LibDockScore)
LRRK2(5OP4)	Britanin	−7.3	1.957	92.8351
CXCR2(6KVA)	Britanin	−1.5	2.151	87.7261
DPP4(4L72)	Britanin	−7.2	30.245	67.1245
HMOX1(1DVE)	Britanin	−7.6	1.613	103.552
MAPK8(4G1W)	Britanin	−7.4	1.862	95.0942
MAPK14(6SFO)	Britanin	−7.7	4.504	95.0706

high-fat group, the mice in the treatment group (Britanin) exhibited significant reductions in body weight, liver weight, and liver index (Figure 6A−C). Furthermore, liver function indicators were examined, and the results showed that compared to the control group, the levels of serum ALT and AST were significantly increased in the high-fat group (Figure 6D,E). However, after Britanin treatment, the levels of AST and ALT were significantly decreased. Histological examination of liver tissue sections stained with HE demonstrated that Britanin treatment effectively alleviated the hepatic steatosis induced by a high-fat diet. These results collectively indicate that Britanin can ameliorate liver injury in mice with high-fat diet-induced NAFLD.

Britanin Inhibits NAFLD in High-Fat Diet-Fed Mice by Reducing Hyperlipidemia and Hepatic Lipid Accumulation. To assess the effect of Britanin on hyperlipidemia in

https://doi.org/10.1021/acsomega.3c08968
ACS Omega 2024, 9, 8274−8286

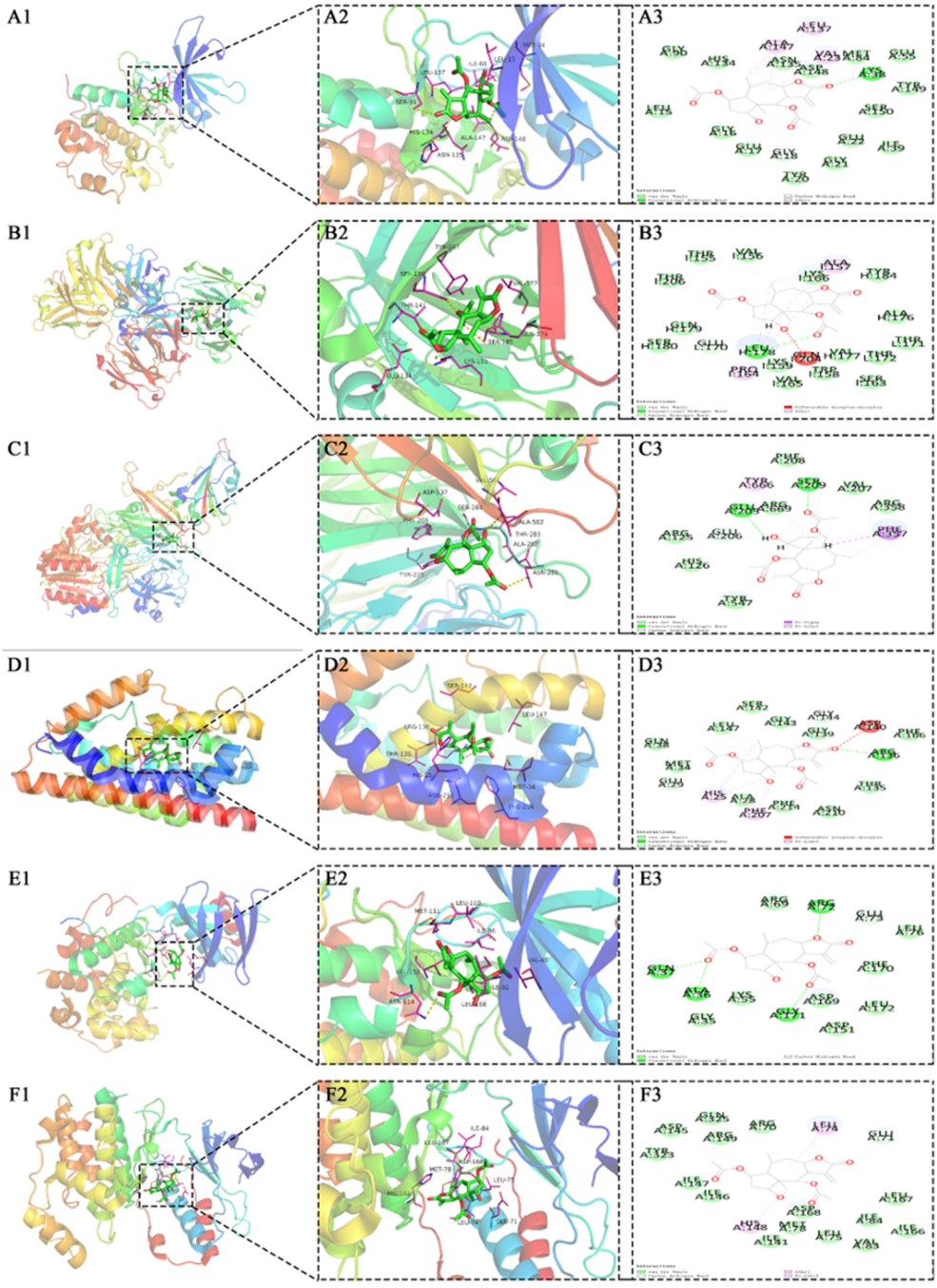

Figure 5. Molecular docking models. (A1) Macroscopic 3D molecular docking model of LRRK2-Britanin. (A2) Microscopic 3D molecular docking model of LRRK2-Britanin. (A3) 2D molecular docking model of LRRK2-Britanin. (B1) Macroscopic 3D molecular docking model of CXCR2-Britanin. (B2) Microscopic 3D molecular docking model of CXCR2-Britanin. (B3) 2D molecular docking model of CXCR2-Britanin. (C1) Macroscopic 3D molecular docking model of DPP4-Britanin. (C2) Microscopic 3D molecular docking model of DPP4-Britanin. (C3) 2D molecular docking model of DPP4-Britanin. (D1) Macroscopic 3D molecular docking model of HMOX1-Britanin. (D2) Microscopic 3D molecular docking model of HMOX1-Britanin. (D3) 2D molecular docking model of HMOX1-Britanin. (E1) Macroscopic 3D molecular docking model of MAPK8-Britanin. (E2) Microscopic 3D molecular docking model of MAPK8-Britanin. (E3) 2D molecular docking model of MAPK8-Britanin. (F1) Macroscopic 3D molecular docking model of MAPK14-Britanin. (F2) Microscopic 3D molecular docking model of MAPK14-Britanin. (F3) 2D molecular docking model of MAPK14-Britanin.

mice with NAFLD, we first examined the levels of TC, TG, HDL-c, and LDL-c in the serum. The results showed that after Britanin treatment, the levels of TC, TG, and LDL-c in the serum were significantly decreased (Figure 7A−D). Conversely, the level of HDL-c was significantly increased, suggesting that Britanin decreased the serum lipid profiles in NAFLD mice. Furthermore, we performed Oil Red O staining on mouse liver tissue (Figure 7E) and found that Britanin could alleviate lipid accumulation in the liver. Numerous studies demonstrated that the AMPK/SREBP1c pathway plays a key role in the regulation of hepatic lipid accumulation in NAFLD mice.[24,25] To further investigate the inhibitory effect of Britanin on hepatic lipid accumulation, we examined the phosphorylation levels of AMPK and the expression levels of SREBP1c. The results

https://doi.org/10.1021/acsomega.3c08968
ACS Omega 2024, 9, 8274−8286

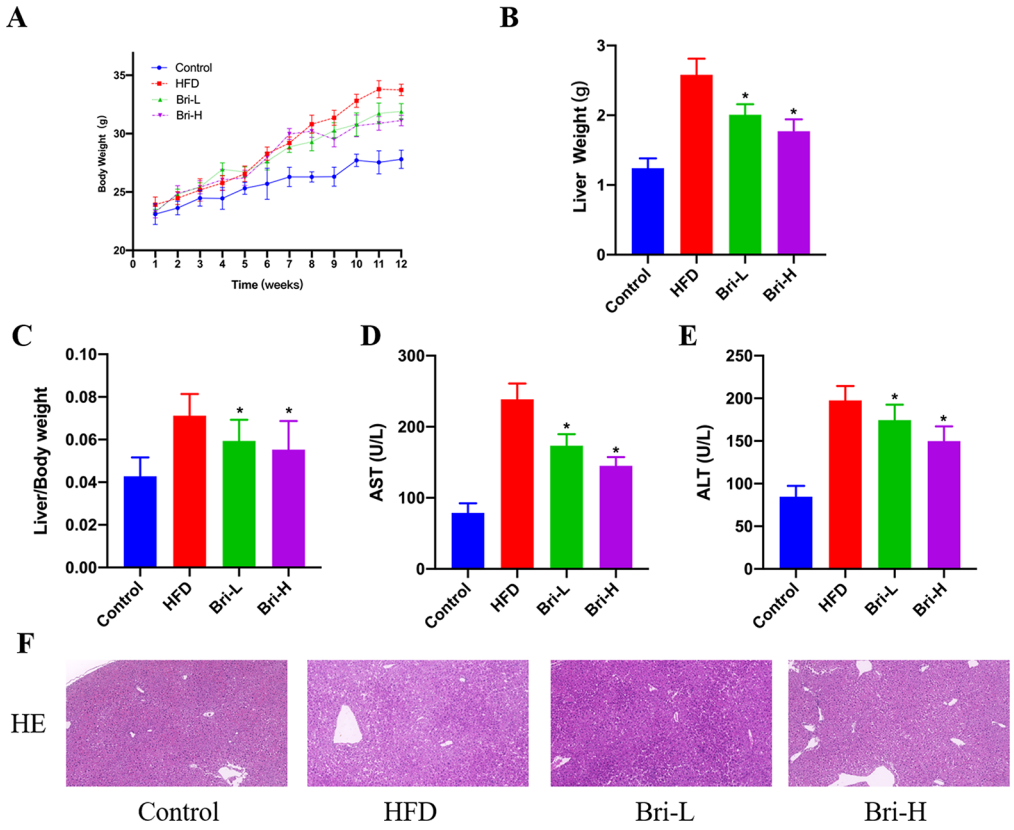

Figure 6. Effects of Britanin on hepatic injury in a high-fat diet-induced NAFLD mouse model. (A) Body weight ($n = 8$). (B) Liver weight ($n = 8$). (C) Liver index ($n = 8$). (D) Serum AST activity ($n = 8$). (E) Serum ALT activity ($n = 8$). (F) Liver H&E staining. Typical images were chosen from each experimental group. Data are shown as mean ± SD. *$P < 0.05$ vs HFD.

demonstrated that Britanin inhibited AMPK phosphorylation and reduced SREBP1c expression (Figure 7F,G). These findings suggest that Britanin suppresses hepatic lipid accumulation in NAFLD mice through the modulation of AMPK phosphorylation and SREBP1c expression.

Britanin Suppresses NAFLD in High-Fat Diet-Fed Mice by Alleviating Oxidative Stress and Apoptosis. Preliminary network pharmacology results indicate that Britanin is involved in oxidative stress responses. Therefore, we next investigated the effect of Britanin on oxidative stress in a NAFLD mouse model. By measuring relevant oxidative stress markers in the serum, we observed that Britanin mitigated the oxidative stress (Figure 8A,B). The results of network pharmacology showed that Britanin and hemeoxygenase-1 (HO-1) were the most stable. It has been reported that enhanced HO-1 expression is involved in the alleviation of oxidative stress during NAFLD progression.[26,27] Therefore, the WB assay was used to detect the level of HO-1, and it was found that the level of HO-1 protein increased significantly after Britanin treatment (Figure 8C). It has been shown that inhibition of apoptosis can alleviate the progression and development of NAFLD. The GO enrichment analysis suggested that Britanin is involved in regulating apoptosis. Further investigation through Western blotting and immunohistochemistry confirmed (Figure 8D,E) that Britanin inhibits the levels of Caspase3 and Bax while upregulating the level of Bcl2. These findings collectively suggest that Britanin ameliorates the development of NAFLD by attenuating hepatic oxidative stress and apoptosis.

DISCUSSION

Recently, a rising number of interconnected investigations and inquiries have focused on conventional pharmacological methods. Although traditional pharmacological approaches have unveiled the pharmacology and mechanisms of drugs, they face challenges in elucidating the intricate interactions and molecular processes occurring between pharmaceuticals and the human body.[28,29] Leveraging the advancements in systems biology and multidimensional pharmacology, network pharmacology amalgamates biological networks with drug actions. It scrutinizes the correlation between drugs and nodes or network modules within the network, employing a multicomponent and multitarget action approach. The current study demonstrated the effects of Britanin on the treatment of NAFLD and revealed the underlying mechanism by integrating pharmaco-bioinformatics approaches and experimental verification. Our findings showed that Britanin had a high affinity for HO-1, according to network pharmacology and molecular docking assays. Moreover, Britanin significantly alleviated oxidative stress by inhibiting HO-1 expression in NAFLD mice. Besides, we also found that Britanin inhibited the development of NAFLD in high-fat diet-fed mice by attenuating liver damage and hepatic lipid accumulation through decreasing serum ALT and AST levels and suppressing the AMPK/SREBP1c pathway. Additionally, Britanin protected against NAFLD via inhibiting apoptosis by downregulating Caspase3 and the Bax/Bcl2 ratio.

NAFLD, a prevalent chronic liver disorder, is intricately linked to dyslipidemia, insulin resistance, obesity, and metabolic syndrome.[30] Although the exact pathogenesis and progression of NAFLD remain elusive, the accumulation of excess lipids in the

https://doi.org/10.1021/acsomega.3c08968
ACS Omega 2024, 9, 8274−8286

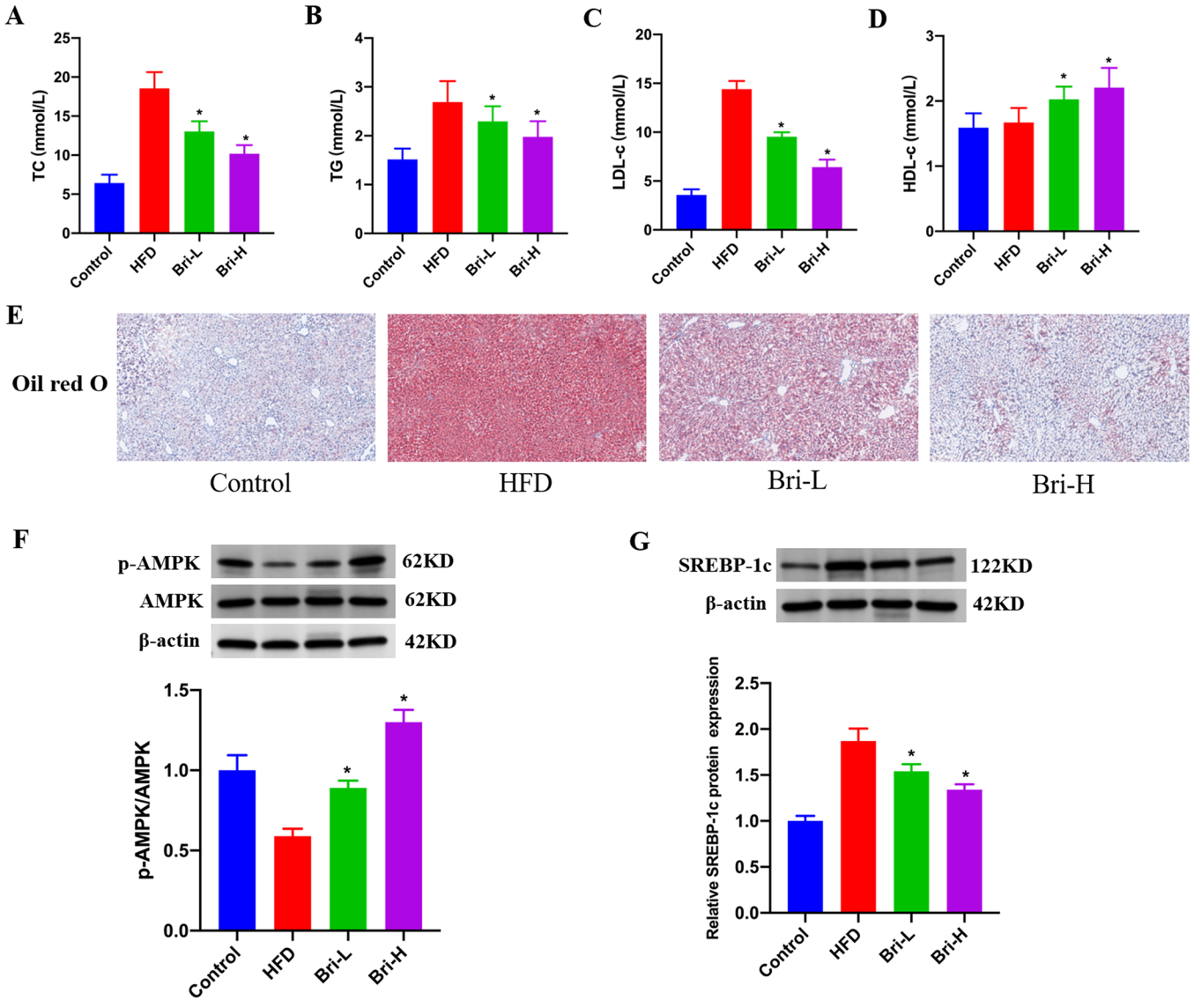

Figure 7. Effects of Britanin on lipid accumulation in a high-fat diet-induced NAFLD mouse model. (A) Serum TC levels ($n = 8$). (B) Serum TG levels ($n = 8$). (C) Serum LDL-c levels ($n = 8$). (D) Serum HDL-c levels ($n = 8$). (E) Liver Oil Red O staining. Typical images were chosen from each experimental group. (F) Hepatic protein expression of p-AMPK and AMPK ($n = 8$). (G) Hepatic protein expression of SREBP-1c ($n = 8$). Data are shown as mean ± SD. *$P < 0.05$ vs HFD.

liver acts as a precursor to steatosis. This, in turn, triggers the generation of lipid peroxidation and engenders lipid-induced toxicity within hepatocytes.[31] Ongoing drug development endeavors predominantly revolve around modulating lipid and glucose metabolism while mitigating oxidative stress damage to the liver.[32] Nevertheless, a universally sanctioned drug for NAFLD treatment has yet to emerge. Although there is currently no specific effective treatment for NAFLD, some traditional Chinese medicine, such as curcumin,[33] Lingguizhugan Decoction,[34] and spleen-strengthening and liver-draining formula,[35] have been in clinical trials. In this study, experimental NAFLD was induced in mice through a high-fat diet. The administration of Britanin was found to attenuate oxidative stress, ameliorate liver injury, and curtail hepatic lipid accumulation in mice subjected to a high-fat diet. These findings unequivocally underscore the potential of Britanin as a promising and novel candidate for NAFLD therapy. Of note, positive drugs are required in animal biological effect experiments. Despite the current constraint on including positive drugs in our experiments, we will conduct positive drug studies to further verify the effect of Britanin on NAFLD in future studies.

Grounded in the concept of component synergy, Traditional Chinese medicine employs a therapeutic approach that spans multiple effects, pathways, and targets, closely aligning with the principles of network pharmacology theory and methodology.[36] Recently, the exploration of Traditional Chinese medicine has significantly embraced network pharmacology to anticipate biologically active constituents and elucidate intricate molecular targets.[37,38] Also, Britanin plays a protective role in liver diseases. For example, Britanin induces apoptosis of hepatocellular carcinoma cells via downregulating the antiapoptotic protein Bcl-2 expression, upregulating the pro-apoptotic protein Bax expression, and suppressing the activation of NF-κB.[39] Consequently, our study harnessed network pharmacology to forecast potential molecular targets and dissect the conceivable mechanism through which Britanin mitigates NAFLD. The network pharmacology and molecular docking results identified HO-1 as the most key target for Britanin against NAFLD.

https://doi.org/10.1021/acsomega.3c08968
ACS Omega 2024, 9, 8274−8286

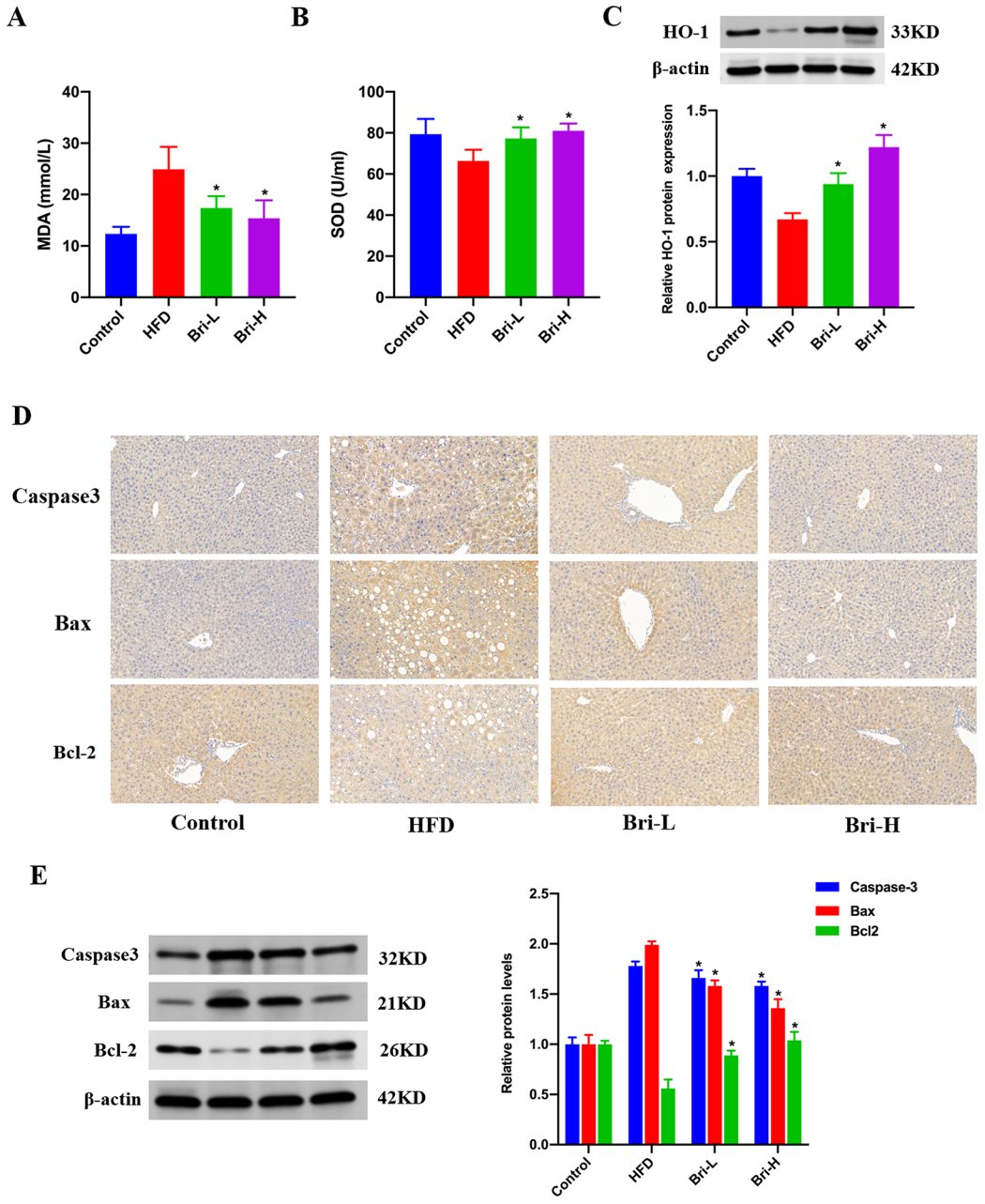

Figure 8. Effects of Britanin on oxidative stress and apoptosis in a high-fat diet-induced NAFLD mouse model. (A) Serum MDA activity (n = 8). (B) Serum SOD activity (n = 8). (C) Hepatic protein expression of HO-1 (n = 8). (D) Liver immunohistochemistry staining. (E) Hepatic protein expression of Caspase3, Bax, and Bcl2. Data are shown as mean ± SD. *P < 0.05 vs HFD.

Decreased hepatic HO-1 expression was reported to improve oxidative stress in the liver and ameliorate the development of NAFLD.[40,41] Importantly, our findings showed that Britanin inhibited oxidative stress by downregulating the level of HO-1 expression. Moreover, the AMPK/SREBP1c pathway that is correlated with lipid metabolism was shown to participate in the Britanin-provided alleviation on NAFLD. In addition, our studies also showed that Britanin decreased Caspase3 expression and the Bax/Bcl2 ratio, thereby inhibiting apoptosis. Taken together, these studies suggest that Britanin has great therapeutic potential and benefits for NAFLD.

CONCLUSIONS

In conclusion, our investigation employed a multifaceted approach encompassing molecular docking, experimental validation, and pharmaco-bioinformatics techniques to corroborate the targets of Britanin and elucidate its potential mechanisms in effectively suppressing NAFLD. Our findings demonstrate that Britanin exerts its influence on NAFLD by mitigating liver injury, curbing hyperlipidemia and hepatic lipid accumulation, and alleviating oxidative stress and apoptosis. This comprehensive methodology underpins the current study, presenting a promising alternative therapeutic avenue characterized by low toxicity. This approach holds the potential for stand-alone use or synergistic integration with other medications for the treatment of NAFLD.

https://doi.org/10.1021/acsomega.3c08968
ACS Omega 2024, 9, 8274−8286

AUTHOR INFORMATION

Corresponding Author

Chuangjie Cao − *Department of Pathology, the First Affiliated Hospital, Hengyang Medical School, University of South China, Hengyang, Hunan Province 421001, China*; Email: Caochj@mail2.sysu.edu.cn

Authors

Chengyun Dou − *Department of Infectious Diseases, the First Affiliated Hospital, Hengyang Medical School, University of South China, Hengyang, Hunan Province 421001, China*; orcid.org/0009-0000-0123-3453

Hongbo Zhu − *Department of Medical Oncology, the First Affiliated Hospital, Hengyang Medical School, University of South China, Hengyang, Hunan Province 421001, China*

Xia Xie − *Department of Infectious Diseases, the First Affiliated Hospital, Hengyang Medical School, University of South China, Hengyang, Hunan Province 421001, China*

Cuiqin Huang − *Department of Pathology, the First Affiliated Hospital, Hengyang Medical School, University of South China, Hengyang, Hunan Province 421001, China*

Complete contact information is available at: https://pubs.acs.org/10.1021/acsomega.3c08968

Author Contributions

C.J.C. designed and conceived the experiments; C.Y.D. and C.J.C. wrote the main manuscript text; C.Y.D. prepared Figures 1−4 and 8; H.B.Z. prepared Figure 5 and helped on the data collection and analysis; X.X. prepared Figure 6; C.Q.H. prepared Figure 5. All authors reviewed the manuscript.

Notes

The authors declare no competing financial interest.

ACKNOWLEDGMENTS

The authors gratefully acknowledge the Scientific Research Project of Health Commission of Hunan Province of China (Grant/Award Number 202103082238 and 202104082246).

REFERENCES

(1) Devarbhavi, H.; Asrani, S. K.; Arab, J. P.; Nartey, Y. A.; Pose, E.; Kamath, P. S. Global burden of liver disease: 2023 update. *Journal of hepatology* **2023**, *79* (2), 516−537.

(2) McPherson, S.; Armstrong, M. J.; Cobbold, J. F.; Corless, L.; Anstee, Q. M.; Aspinall, R. J.; Barclay, S. T.; Brennan, P. N.; Cacciottolo, T. M.; Goldin, R. D.; Hallsworth, K.; Hebditch, V.; Jack, K.; Jarvis, H.; Johnson, J.; Li, W.; Mansour, D.; McCallum, M.; Mukhopadhya, A.; Parker, R.; Ross, V.; Rowe, I. A.; Srivastava, A.; Thiagarajan, P.; Thompson, A. I.; Tomlinson, J.; Tsochatzis, E. A.; Yeoman, A.; Alazawi, W. Quality standards for the management of non-alcoholic fatty liver disease (NAFLD): consensus recommendations from the British Association for the Study of the Liver and British Society of Gastroenterology NAFLD Special Interest Group. *Lancet Gastroenterol Hepatol* **2022**, *7* (8), 755−769.

(3) Allen, A. M.; Hicks, S. B.; Mara, K. C.; Larson, J. J.; Therneau, T. M. The risk of incident extrahepatic cancers is higher in non-alcoholic fatty liver disease than obesity - A longitudinal cohort study. *Journal of hepatology* **2019**, *71* (6), 1229−1236.

(4) Targher, G.; Byrne, C. D.; Tilg, H. NAFLD and increased risk of cardiovascular disease: clinical associations, pathophysiological mechanisms and pharmacological implications. *Gut* **2020**, *69* (9), 1691−1705.

(5) Tilg, H.; Targher, G. NAFLD-related mortality: simple hepatic steatosis is not as 'benign' as thought. *Gut* **2021**, *70* (7), 1212−1213.

(6) Simon, T. G.; Roelstraete, B.; Khalili, H.; Hagström, H.; Ludvigsson, J. F. Mortality in biopsy-confirmed nonalcoholic fatty liver disease: results from a nationwide cohort. *Gut* **2021**, *70* (7), 1375−1382.

(7) Eslam, M.; Valenti, L.; Romeo, S. Genetics and epigenetics of NAFLD and NASH: Clinical impact. *Journal of hepatology* **2018**, *68* (2), 268−279.

(8) Powell, E. E.; Wong, V. W.; Rinella, M. Non-alcoholic fatty liver disease. *Lancet (London, England)* **2021**, *397* (10290), 2212−2224.

(9) Ferguson, D.; Finck, B. N. Emerging therapeutic approaches for the treatment of NAFLD and type 2 diabetes mellitus. *Nat. Rev. Endocrinol* **2021**, *17* (8), 484−495.

(10) Younossi, Z. M.; Golabi, P.; de Avila, L.; Paik, J. M.; Srishord, M.; Fukui, N.; Qiu, Y.; Burns, L.; Afendy, A.; Nader, F. The global epidemiology of NAFLD and NASH in patients with type 2 diabetes: A systematic review and meta-analysis. *Journal of hepatology* **2019**, *71* (4), 793−801.

(11) Targher, G.; Corey, K. E.; Byrne, C. D.; Roden, M. The complex link between NAFLD and type 2 diabetes mellitus - mechanisms and treatments. *Nat. Rev. Gastroenterol Hepatol* **2021**, *18* (9), 599−612.

(12) Katsiki, N.; Mikhailidis, D. P.; Mantzoros, C. S. Non-alcoholic fatty liver disease and dyslipidemia: An update. *Metabolism: clinical and experimental* **2016**, *65* (8), 1109−23.

(13) Stefan, N.; Häring, H. U.; Cusi, K. Non-alcoholic fatty liver disease: causes, diagnosis, cardiometabolic consequences, and treatment strategies. *lancet. Diabetes & endocrinology* **2019**, *7* (4), 313−324.

(14) Zhou, X. D.; Cai, J.; Targher, G.; Byrne, C. D.; Shapiro, M. D.; Sung, K. C.; Somers, V. K.; Chahal, C. A. A.; George, J.; Chen, L. L.; Zhou, Y.; Zheng, M. H. Metabolic dysfunction-associated fatty liver disease and implications for cardiovascular risk and disease prevention. *Cardiovasc. Diabetol.* **2022**, *21* (1), 270.

(15) Yang, L.; Wang, X.; Hou, A.; Zhang, J.; Wang, S.; Man, W.; Yu, H.; Zheng, S.; Wang, Q.; Jiang, H.; Kuang, H. A review of the botany, traditional uses, phytochemistry, and pharmacology of the Flos Inulae. *J. Ethnopharmacol* **2021**, *276*, No. 114125.

(16) Zhang, J.; Zhang, M.; Zhang, W. H.; Zhu, Q. M.; Ning, J.; Huo, X. K.; Xiao, H. T.; Sun, C. P. Total terpenoids of Inula japonica activated the Nrf2 receptor to alleviate the inflammation and oxidative stress in LPS-induced acute lung injury. *Phytomedicine: international journal of phytotherapy and phytopharmacology* **2022**, *107*, No. 154377.

(17) Bae, W. Y.; Lee, D. U.; Yu, H. S.; Lee, N. K.; Paik, H. D. Fermentation of Inula britannica using Lactobacillus plantarum SY12 increases of epigallocatechin gallate and attenuates toxicity. *Food Chem.* **2023**, *429*, No. 136844.

(18) Li, K.; Zhou, Y.; Chen, Y.; Zhou, L.; Liang, J. A novel natural product, britanin, inhibits tumor growth of pancreatic cancer by suppressing nuclear factor-κB activation. *Cancer Chemother Pharmacol* **2020**, *85* (4), 699−709.

(19) Bae, W. Y.; Kim, H. Y.; Park, E. H.; Kim, K. T.; Paik, H. D. Improved in vitro antioxidant properties and hepatoprotective effects of a fermented Inula britannica extract on ethanol-damaged HepG2 cells. *Mol. Biol. Rep* **2019**, *46* (6), 6053−6063.

(20) Wu, G.; Zhu, L.; Yuan, X.; Chen, H.; Xiong, R.; Zhang, S.; Cheng, H.; Shen, Y.; An, H.; Li, T.; Li, H.; Zhang, W. Britanin Ameliorates Cerebral Ischemia-Reperfusion Injury by Inducing the Nrf2 Protective Pathway. *Antioxidants & redox signaling* **2017**, *27* (11), 754−768.

(21) Kim, S. G.; Lee, E.; Park, N. Y.; Park, H. H.; Jeong, K. T.; Kim, K. J.; Lee, Y. J.; Jin, M.; Lee, E. Britanin attenuates ovalbumin-induced airway inflammation in a murine asthma model. *Arch Pharm. Res.* **2016**, *39* (7), 1006−12.

(22) Yu, H. S.; Kim, W. J.; Bae, W. Y.; Lee, N. K.; Paik, H. D. Inula britannica Inhibits Adipogenesis of 3T3-L1 Preadipocytes via Modulation of Mitotic Clonal Expansion Involving ERK 1/2 and Akt Signaling Pathways. *Nutrients* **2020**, *12* (10), 3037 DOI: 10.3390/nu12103037.

(23) Shan, J. J.; Yang, M.; Ren, J. W. Anti-diabetic and hypolipidemic effects of aqueous-extract from the flower of Inula japonica in alloxan-induced diabetic mice. *Biol. Pharm. Bull.* **2006**, *29* (3), 455−9.

(24) Shen, B.; Wang, Y.; Cheng, J.; Peng, Y.; Zhang, Q.; Li, Z.; Zhao, L.; Deng, X.; Feng, H. Pterostilbene alleviated NAFLD via AMPK/mTOR signaling pathways and autophagy by promoting Nrf2. *Phytomedicine: international journal of phytotherapy and phytopharmacology* **2023**, *109*, No. 154561.
(25) Liu, X.; Hu, M.; Ye, C.; Liao, L.; Ding, C.; Sun, L.; Liang, J.; Chen, Y. Isosilybin regulates lipogenesis and fatty acid oxidation via the AMPK/SREBP-1c/PPARα pathway. *Chem. Biol. Interact* **2022**, *368*, No. 110250.
(26) Li, J.; Wang, T.; Liu, P.; Yang, F.; Wang, X.; Zheng, W.; Sun, W. Hesperetin ameliorates hepatic oxidative stress and inflammation via the PI3K/AKT-Nrf2-ARE pathway in oleic acid-induced HepG2 cells and a rat model of high-fat diet-induced NAFLD. *Food & function* **2021**, *12* (9), 3898−3918.
(27) Malaguarnera, L.; Madeddu, R.; Palio, E.; Arena, N.; Malaguarnera, M. Heme oxygenase-1 levels and oxidative stress-related parameters in non-alcoholic fatty liver disease patients. *Journal of hepatology* **2005**, *42* (4), 585−91.
(28) Liu, X.; Wu, W. Y.; Jiang, B. H.; Yang, M.; Guo, D. A. Pharmacological tools for the development of traditional Chinese medicine. *Trends Pharmacol. Sci.* **2013**, *34* (11), 620−8.
(29) Zhang, R.; Zhu, X.; Bai, H.; Ning, K. Network Pharmacology Databases for Traditional Chinese Medicine: Review and Assessment. *Front. Pharmacol.* **2019**, *10*, 123.
(30) Targher, G.; Tilg, H.; Byrne, C. D. Non-alcoholic fatty liver disease: a multisystem disease requiring a multidisciplinary and holistic approach. *Lancet Gastroenterol Hepatol* **2021**, *6* (7), 578−588.
(31) Mota, M.; Banini, B. A.; Cazanave, S. C.; Sanyal, A. J. Molecular mechanisms of lipotoxicity and glucotoxicity in nonalcoholic fatty liver disease. *Metabolism: clinical and experimental* **2016**, *65* (8), 1049−61.
(32) Friedman, S. L.; Neuschwander-Tetri, B. A.; Rinella, M.; Sanyal, A. J. Mechanisms of NAFLD development and therapeutic strategies. *Nature medicine* **2018**, *24* (7), 908−922.
(33) Saadati, S.; Sadeghi, A.; Mansour, A.; Yari, Z.; Poustchi, H.; Hedayati, M.; Hatami, B.; Hekmatdoost, A. Curcumin and inflammation in non-alcoholic fatty liver disease: a randomized, placebo controlled clinical trial. *BMC Gastroenterol.* **2019**, *19* (1), 133.
(34) Dai, L.; Xu, J.; Liu, B.; Dang, Y.; Wang, R.; Zhuang, L.; Li, D.; Jiao, L.; Wang, J.; Zhang, L.; Zhong, L. L. D.; Zhou, W.; Ji, G. Lingguizhugan Decoction, a Chinese herbal formula, improves insulin resistance in overweight/obese subjects with non-alcoholic fatty liver disease: a translational approach. *Frontiers of medicine* **2022**, *16* (5), 745−759.
(35) Hui, D.; Liu, L.; Azami, N. L. B.; Song, J.; Huang, Y.; Xu, W.; Wu, C.; Xie, D.; Jiang, Y.; Bian, Y.; Sun, M. The spleen-strengthening and liver-draining herbal formula treatment of non-alcoholic fatty liver disease by regulation of intestinal flora in clinical trial. *Front. Endocrinol.* **2022**, *13*, No. 1107071.
(36) Jiang, L.; Shi, Z.; Yang, Y. Network Pharmacology-Based Approach to Investigate the Molecular Targets of Rhubarb for Treating Cancer. *J. Evidence-Based Complementary Altern. Med.* **2021**, *2021*, No. 9945633.
(37) Jiao, X.; Jin, X.; Ma, Y.; Yang, Y.; Li, J.; Liang, L.; Liu, R.; Li, Z. A comprehensive application: Molecular docking and network pharmacology for the prediction of bioactive constituents and elucidation of mechanisms of action in component-based Chinese medicine. *Comput. Biol. Chem.* **2021**, *90*, No. 107402.
(38) Wang, X.; Wang, Z. Y.; Zheng, J. H.; Li, S. TCM network pharmacology: A new trend towards combining computational, experimental and clinical approaches. *Chin J. Nat. Med.* **2021**, *19* (1), 1−11.
(39) Li, H.; Du, G.; Yang, L.; Pang, L.; Zhan, Y. The Antitumor Effects of Britanin on Hepatocellular Carcinoma Cells and its Real-Time Evaluation by In Vivo Bioluminescence Imaging. *Anticancer Agents Med. Chem.* **2020**, *20* (9), 1147−1156.
(40) Ogino, N.; Miyagawa, K.; Nagaoka, K.; Matsuura-Harada, Y.; Ogino, S.; Kusanaga, M.; Oe, S.; Honma, Y.; Harada, M.; Eitoku, M.; Suganuma, N.; Ogino, K. Role of HO-1 against Saturated Fatty Acid-Induced Oxidative Stress in Hepatocytes. *Nutrients* **2021**, *13* (3), 993 DOI: 10.3390/nu13030993.
(41) Li, D.; Yuan, X.; Dong, S.; Al-Dhamin, Z.; Du, J.; Fu, N.; Nan, Y. Heme oxygenase-1 prevents non-alcoholic steatohepatitis through modulating mitochondrial quality control. *Acta Physiol.* **2023**, *237* (3), No. e13918.

https://doi.org/10.1021/acsomega.3c08968
ACS Omega 2024, 9, 8274−8286